Mitochondrion 24 (2015) 113–121

Contents lists available at ScienceDirect

Mitochondrion

journal homepage: www.elsevier.com/locate/mito

Impaired mitochondrial protein synthesis in head and neck squamous cell carcinoma

Emine C. Koc [a,*,1], Ebru Haciosmanoglu [a,1], Pier Paolo Claudio [a,b,2], Allison Wolf [a], Luigi Califano [c], Marco Friscia [c], Antonio Cortese [d], Hasan Koc [e]

[a] Department of Biochemistry and Microbiology, Joan C. Edwards School of Medicine, Marshall University, Huntington, WV 25755, United States
[b] Department of Surgery, Joan C. Edwards School of Medicine, Marshall University, Huntington, WV 25755, United States
[c] Department of Maxillo-Facial Surgery, University of Naples "Federico II", Italy
[d] Department of Medicine and Surgery, Unit of Maxillofacial Surgery, University of Salerno, Salerno, Italy
[e] Department of Pharmaceutical Science and Research, School of Pharmacy, Marshall University, Huntington, WV 25755, United States

ARTICLE INFO

Article history:
Received 17 April 2015
Received in revised form 24 July 2015
Accepted 29 July 2015
Available online 1 August 2015

Keywords:
Oxidative phosphorylation defect
Mitochondrial translation
Mitochondrial protein synthesis
Mitochondrial ribosomal proteins
MRPL11
Head and neck cancer
Squamous cell carcinoma

ABSTRACT

Human head and neck squamous cell carcinoma (HNSCC) is the sixth most common cancer type worldwide, possibly due to the significant role of alcohol and tobacco use in its development. Underlying most cancers are defects in mitochondrial functions such as energy metabolism and apoptosis. In fact, the mutations in mitochondrial DNA (mtDNA), which encode proteins for oxidative phosphorylation (OXPHOS), have been associated with human head and neck cancers. Here, we investigated the changes in the expression of OXPHOS complexes and the contribution of the defects in mitochondrial translation in the progression of HNSCC. Western blot analyses of the several stage IVA HNSCC primary tumors have shown reduction in the expression of COII and ATP5A of the OXPHOS complexes IV and V subunits, respectively. On the other hand, expression of the majority of the OXPHOS subunits, except complex II SDHB subunit, was impaired in a patient with a stage IV tumor with a regional lymph node. Interestingly, an overall reduction in one of the mitochondrial-encoded subunits of the complex IV, COII, accentuated a possible defect in mitochondrial translation machinery in two of the stage IVA tumors. Evidence provided in this study suggests for the first time that the mitochondrial translation defect(s) could be due to a decrease in the expression of one of the essential mitochondrial ribosomal proteins, MRPL11, in head and neck tumor biopsies. We also observed an acquired mitochondrial translation deficiency in the HN8 cell line derived from a lymph node metastasis but not in the HN22 cells derived from the primary tumor of the same patient. These seminal observations suggest that the mitochondrial translation machinery deserves further investigation for accurate molecular assessment and treatment of HNSCC.

1. Introduction

The two vital roles of mitochondria are the generation of energy by oxidative phosphorylation (OXPHOS) and induction of apoptosis by releasing several critical pro-apoptotic proteins. Changes in both mitochondrial energy metabolism and apoptosis are described as the hallmarks of cancer (Brandon et al., 2006; Wallace, 2012; Hanahan and Weinberg, 2011; Chandra and Singh, 2011). Defects in these processes promote cancer cell growth predominately by producing energy through aerobic glycolysis and bypassing intrinsic apoptotic pathways.

Energy metabolism by OXPHOS is supported by nuclear and mitochondrial-encoded genes in eukaryotes. The mitochondrial genome is 16.5 kb circular DNA (mtDNA) and contains only 37 genes, 13 of which are involved in the synthesis of mitochondrial-encoded proteins. The remaining 24 genes encode for two rRNAs and 22 tRNAs. Mitochondria also contain their own specific ribosome, which is composed of two mitochondrially encoded rRNAs, the 12S and 16S, and about 85 nuclear-encoded mitochondrial ribosomal proteins (MRPs) as described in our recent studies (Koc et al., 2013). Mitochondrial translation machinery is absolutely essential for the synthesis of 13 core components of the OXPHOS complexes, and, therefore, energy production by this process. In a recent seminal study, 55% of the mitochondrial translation components, mainly MRPs, have been shown to be essential for the retention of the mitochondrial genome in yeast (Zhang and Singh, 2014). In addition to their roles in protein synthesis, several MRPs have been found to be involved in apoptosis (Han et al., 2010; Kissil et al., 1995; Miller et al., 2008; Mukamel and Kimchi, 2004; Carim et al., 1999; Levshenkova et al., 2004; Koc et al., 2001a). We have shown that the two well-known pro-apoptotic MRPs, death associated protein 3 (DAP3, also known as MRPS29) and MRPS30, are components of the small subunit of the mitochondrial ribosome (Han et al., 2010; Miller et al., 2008; Koc et al., 2001a).

* Corresponding author.
E-mail address: koce@marshall.edu (E.C. Koc).
[1] Equally contributed to the manuscript.
[2] Current affiliation: National Center for Natural Products Research and Department of BioMolecular Sciences, School of Pharmacy, University of Mississippi, University, MS 38677, United States. Department of Radiation Oncology, University of Mississippi Medical Center, Jackson, MS 39216, United States.

http://dx.doi.org/10.1016/j.mito.2015.07.123
1567-7249/

Mutations in mitochondrial genes have been associated with head and neck squamous cell carcinomas (HNSCC). Specifically, the mitochondrial-encoded subunits of complex IV (COI, COII, and COIII) are found to be the most commonly mutated genes in HNSCC patients (Challen et al., 2011; Dasgupta et al., 2010; Kim et al., 2006). In addition to these mtDNA mutations, nuclear genes encoding for proteins responsible for mitochondrial biogenesis are also reported to be involved in HNSCC. Furthermore, aberrant expression of the mRNAs of mitochondrial ribosomal proteins (MRPs) has been associated with various cancers, including head and neck cancer (Cavalieri et al., 2007; Huang et al., 2011; Milne et al., 2010; Sotgia et al., 2012; Stacey et al., 2008; Yoo et al., 2005). Interestingly, the MRPs MRPL11 and MRPL21 were among the six aberrantly expressed genes as detected by microarray analysis of normal and primary HNSCC tissues (Sugimoto et al., 2009).

In this study, we investigated the expression of OXPHOS complexes at steady-state levels and discovered defective expression of their mitochondrial- and nuclear-encoded components in HNSCC. Moreover, the expression of MRPL11, an essential protein of the large subunit of the mitochondrial ribosome, is altered in tumor tissues, possibly resulting in impaired synthesis of OXPHOS subunits. Our studies strongly indicate that impaired mitochondrial translation could be one of the underlying reasons for metabolic transformation of tumors in head and neck cancers.

2. Materials and methods

2.1. HNSCC tumor samples

The HNSCC samples were derived from patients who underwent surgical resection as first-line treatment at the Department of Maxillo-Facial Surgery, University of Naples "Federico II," Naples, Italy. Patients signed an informed consent for the study, which was reviewed by the Institutional Review Board. Staging was carried out according to the tumor-node-metastasis classification, and the tumors were graded as: well (G1), intermediate (G2), and poorly differentiated (G3). Normal, paired tissues were used as a control. Only patients with primary oral cavity tumors who had not undergone any previous irradiation or chemotherapeutic treatment were included in the study. Six different patient tissue samples used were as follows: sample 1, squamous cell carcinoma, oral pavement; sample 2, squamous cell carcinoma, tongue; sample 3, squamous cell carcinoma, infiltrating mandible; sample 4, squamous cell carcinoma, trigon region; sample 5, squamous cell carcinoma, tongue; sample 6 L, squamous cell carcinoma, left cheek; and sample 6R, squamous cell carcinoma, right cheek. Tumor samples 6 L and 6R were taken from the same patient. Grade and stage of tumor biopsies are summarized in Table 1.

Protein lysates used in Western blot analysis were obtained by resuspension and sonication of tumor samples in RIPA. Supernatants obtained from the lysates were precipitated by the addition of 80% cold acetone (v/v) for 1 h at −80 °C. Protein pellets were collected by centrifugation at 14 K rpm for 10 min. and resuspended in RIPA buffer containing 0.5% SDS. The supernatant was collected and used for protein analysis.

2.2. Cell culture

The control cell line, the human adult keratinocyte cell line HaCaT, was obtained from Zen-Bio, Inc (Research Triangle Park, NC). The HN12 cell line was a kind gift from Dr. George Yoo (Karmanos Cancer Center, Wayne State University, OH) after authentication by PCR amplification of short tandem repeats to ensure cell identity. The H8, H13, and HN22 cell lines were kindly provided by Dr. Gutkind (National Institute of Dental and Craniofacial Research, NIH, Bethesda, MD) after authentication by PCR amplification of short tandem repeats to ensure cell identity. Tumor staging characteristics of head and neck cancer cell lines are given in Table 2 (Jeon et al., 2004). Monolayer cultures were maintained in DMEM medium (HyClone, Thermo-Scientific) adjusted to contain 10% fetal bovine serum (FBS) (PAA Laboratories GmbH, Pasching, Austria) and supplemented with 1% penicillin–streptomycin (P/S) (Corning Cellgro, Manassas, VA). HaCaT cells were maintained in Adult Keratinocyte Growth Medium (KM-2) (Zen-Bio, Research Triangle Park, NC). Cells were grown in a humidified incubator at 37 °C and 5% CO_2.

2.3. Western blot analysis

Whole cell lysates obtained from tumor tissue samples and head and neck cancer cell lines outlined above were separated on 12% SDS-PAGE. Proteins were transferred to nitrocellulose membranes, which were probed with appropriate human antibodies against the following proteins at the specified dilutions: OXPHOS ATP5a (1:500), OXPHOS Complex III Subunit (1:500), SDHA (1:2500), SDHB (1:500), Complex IV Subunit II (1:500), Complex I NDUF8 (1:500), HSP60 (1:5000), GAPDH (1:14,000); MRPL11 (1:2500), MRPL40 (1:2500), MRPL47 (1:250 dilution), and MRPS29 (1:500) overnight at 4 °C. The secondary antibodies — mouse and rabbit IgG HRP conjugates — were all used for 1 h at 1:5000 dilutions. The membranes were developed using the protocols provided by the manufacturer.

2.4. [^{35}S]-Methionine pulse labeling of mitochondrial translation products in vivo

Pulse labeling experiments were performed in minimum essential DMEM medium without methionine, glutamine, or cysteine, and dialyzed serum (25 mM Tris–HCl, pH 7.4, 137 mM NaCl, and 10 mM KCl) as indicated in our previous reports (Koc et al., 2013; Yang et al., 2010). Cytoplasmic protein synthesis was arrested by incubating cells with emetine-containing medium for 15 min. In order to label the mitochondrial-encoded proteins, 0.2 mCi/mL of [^{35}S]-methionine-containing medium (Perkin Elmer) was added to the cells. After a 2 hour incubation, cells were lysed in buffer containing the following: 50 mM

Table 1
Clinical data of patients affected by squamous cell carcinoma of the oral cavity.

Patient	Gender	Age	Smoke	Alcohol consumption	Site	Grade	TNM	Stage
1	M	51	Y	Y	Oral pavement, infiltrating cortical mandible bone	G2	T4aN0M0	IVA
2	M	50	Y	Y	Tongue	G1	T2N0M0	II
3	M	49	Y	Y	Oral pavement infiltrating the mandible	G2	T4aN0M0	IVA
4	F	67	Y	N	Retromolar trigon	G2	T4aN2bM0	IVA
5	M	50	Y	Y	Tongue	G1	T2N0M0	II
6L [a]	M	64	Y	Y	Buccal mucosa right side	G1	T1N0M0	I
6R [a]	M	64	Y	Y	Buccal mucosa left side	G2	T3N1M0	III

T: primary tumor.
N: regional lymph nodes.
M: distant metastasis.
[a] Patient 6R and 6L is the same patient, affected by two independent synchronous tumors (one on the left cheek and one on the right cheek).

Table 2
Characterization of HN8, HN12, HN13, and HN22 cell lines.

HNSCC cell line	Site	Origin	TNM	Stage	Tumorigenic	Migration capabilities
HN8[a]	Lymph node metastasis	Oral pavement	T3N2M0	IVA	Yes	Moderate
HN12	Lymph node metastasis	Tongue	T4N1M0	II	Yes	High
HN13	Primary tumor	Tongue	T2N2M0	II	No	Moderate
HN22[a]	Primary tumor	Oral pavement	T3N2M0	IVA	Yes	High

[a] Indicates cell lines derived from the same patient (primary tumor/paired nodal metastasis). Tumor staging of these cell lines was previously reported (Yoo et al., 2005).

Tris–HCl, pH 7.6, 150 mM NaCl, 1 mM EDTA, 1 mM EGTA, 0.1% SDS, and 0.5% NP-40 supplemented with 1 mM PMSF and protease inhibitor cocktail (Sigma-Aldrich). Electrophoresis of whole cell lysates (40 μg) was performed through 12% SDS-PAGE. The gels were dried on 3 MM chromatography paper (Whatman), and the total intensities of the signals were quantified by phosphorimaging analyses. The siRNA-mediated knock-down efficiency of the corresponding mitochondrial ribosomal protein was confirmed with Western blot analysis of whole cell lysates, prepared as stated above.

2.5. Reverse transcription polymerase chain reaction (RT-PCR)

Total RNA was extracted using TRIzol (Invitrogen, Carlsbad, CA) and then converted to cDNA with a High Capacity cDNA Reverse Transcription Kit (Applied Biosystems, Inc, Foster City, CA, USA) using random primers. qRT-PCRs were carried out using RT^{2}Real-Time^{TM} SYBR Green/Rox PCR master mix (SABiosciences, Fredrick, MD, USA) and run on an Applied Biosystems 7000 real-time thermal cycler (Applied Biosystems, Inc). Reactions were carried out in technical triplicates and biological triplicates. Relative expression values were calculated using the ΔΔCt method. The following primer sequences were used: MRPL11 forward 5′-CCCACTAGGCCCAGTGCT-3′ and reverse 5′-GAGGAATGCCTTCCTTGATGTCC-3′; CO-II forward 5′-ATGGACATGCATGCAGC- GCAAGTA-3′ and reverse 5′-CTATAGGGAAGTGCACTTTCCAG-3′; and GAPDH forward 5′-CGACAGTCGAGCCG and reverse 5′-CCAATACGACCA-3′.

Semi-quantitative RT-PCR was performed on four of the Head and Neck cell lines (HaCat, HN8, HN12, and HN22). Total RNA was extracted using TRIzol (Invitrogen, Carlsbad, CA) and then converted to cDNA with a High Capacity cDNA Reverse Transcription Kit (Applied Biosystems, Inc, Foster City, CA, USA) using random primers. Aliquots of 1 μL of the reserve-transcribed cDNA samples were added to 20 μL of a reaction mixture made using Phusion High-Fidelity PCR Kit (New England Biolabs, Ipswich, MA) that contained: 4 μL of 10× buffer with $MgCl_2$, 0.4 μl of 10 mM dNTP mix, 0.4 μl of *Taq* polymerase (Phusion High-Fidelity DNA Polymerase) and 1 μl of each primer. Samples were co-amplified for 29 cycles: denaturation at 98 °C for 30 s, annealing at 60 °C (for 30 s, extension at 72 °C for 1 min and final extension at 72 °C for 10 min). The PCR products (10 μL) were applied to a 1% agarose gel containing 10 μg of ethidium bromide and electrophoresed. The gel was then illuminated on an UV table FOTO/Analyst® Luminary/FX® System (Fotodyne, Hartland, WI, USA). Densitometry analysis was performed using TotalLab Quant (TotalLab Ltd, Newcastle upon Tyne, UK), and then the relative value of the COII band to GAPDH was calculated in each sample. Reactions were carried out in technical triplicates and biological triplicates.

2.6. Wound-healing assays

Cell migration of HN8, HN12, and HN22 cells was determined using a wound-healing assay. HNSCC cells were cultured in 6-well dishes until 90% confluent and then synchronized with DMEM (1% P/S, 0.5% FBS). After synchronizing cells for 24 h, a line was drawn horizontally on the bottom of each well using a permanent marker, and a p200 pipette tip was used to generate 3 vertical scratches per well. Cells were then incubated for 24 h in DMEM (1% P/S, 10% FBS). Scratch sizes were determined with a light inverted microscope (Olympus IX51) at 100× magnification. Six measurements were made per well after 24 h, 1 below and 1 above the horizontal line for each scratch. Images were taken as described above and changes in cell migration were determined by calculating the percent of wound healing. Percent wound healing = $([\text{scratch}_{t\text{-}0\,h} - \text{scratch}_{t\text{-}24\,h}] / \text{scratch}_{t\text{-}0\,h})*100$. Experiments were repeated a minimum of 3 times.

3. Results

3.1. Expression of OXPHOS complexes is impaired in HNSCC tumors and cell lines

Mutations in mtDNA in tumors obtained from HSNCC patients have been reported previously (Dasgupta et al., 2010). However, the effects of these point mutations on the steady-state expression of OXPHOS complexes have not been shown. We first evaluated the expression of the OXPHOS subunits in seven surgically removed tumors obtained from six HNSCC patients (tumor staging given in Table 1) by Western blotting analysis using an OXPHOS antibody cocktail (Fig. 1A). The cocktail contains antibodies for nuclear-encoded subunits of complex V (ATP5A), III (UQCRC2), II (SDHB), I (NDUF8), and the mitochondrial-encoded subunit of complex IV (COII). The tumor samples were also probed with GAPDH antibody as a loading control. Surprisingly, only the complex II subunit, SDHB, was consistently detected in all of the samples, while the expression of the complex V, IV, III, and I subunits were significantly impaired in one of the tumor tissue samples (Fig. 1A). These complexes contain at least one mitochondrial-encoded subunit, while complex II subunits are all nuclear encoded. Therefore, it is possible that the changes observed in the expression of complex I, III, IV, and V subunits could be due to defects in the synthesis of both nuclear- and mitochondrial-encoded components. The only mitochondrial-encoded protein detected in this analysis is the COII subunit of complex IV; the other proteins detected by this antibody are all nuclear-encoded (Fig. 1A). Interestingly, we found that the expression of COII was significantly decreased in the tumor tissue from patient 4 and slightly reduced in patients 1 and 3. Tumors from patients 1, 3, and 4 were stage IVA, grade G2 squamous cellular carcinomas of the oral cavity and of the retromolar trigon, respectively (Table 1). One of the unexpected observations, however, was the overexpression of COII in the tumor obtained from right cheek of patient 6, whereas its expression was significantly reduced in the tumor obtained from the left cheek (Fig. 1A).

The intriguing results obtained in the HNSCC biopsies (Fig. 1A) led us to consider exploration of mitochondrial translation further in head and neck cancer. However, the amounts of tissue samples were limited for a comprehensive analysis of mitochondrial translation products and components. To overcome this limitation we used a normal human adult keratinocyte cell line and several different head and neck (HN) cancer cell lines to perform a more comprehensive analysis of the expression of OXPHOS components.

As shown in Fig. 1B, the majority of the OXPHOS components were equally expressed in the control HaCat and HN cancer cell lines; however, the mitochondrial- and nuclear-encoded subunits of complex IV and I, COII and NDUF8, respectively, were not equally expressed. The reduced expression of COII was only observed in HN8 cells, while the

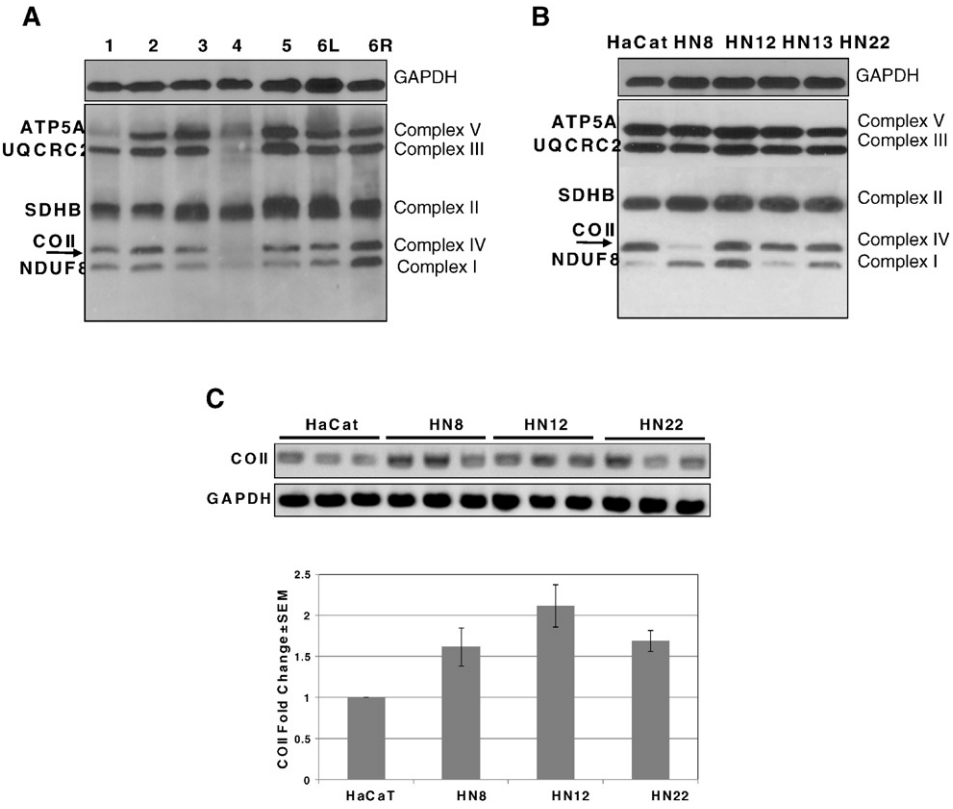

Fig. 1. Mitochondrial oxidative phosphorylation is defective in human head and neck cancers and cell lines. A) Expression of oxidative phosphorylation (OXPHOS) subunits, including SDHA and SDHB (Complex II), ATP5A (Complex IV), UQCRC2 (Complex III), COII (Complex IV), and NDUF8 (Complex I) were detected by Western blot analysis of seven human head and neck tumor biopsies. Tumor biopsies taken from the left (6 L) and right (6R) cheeks of patient # six were labeled as shown. The mitochondrial-encoded subunit COII is marked by an arrow. B) Expression of OXPHOS subunits was evaluated in a normal keratinocyte cell line (HaCat), used as a control, and four HNSCC (HN8, HN12, HN13, and HN22) cell lines by Western blot analysis. The steady state levels of the mitochondrial-encoded subunit of Complex IV (COII, shown by an arrow) are reduced in HN8, HN13, and HN22 cell lines. C) Relative changes in COII mRNA expression were determined by semi quantitative RT-PCR and reported as fold change with respect to changes in GAPDH mRNA expression in HaCat, HN8, HN12, and HN22 cells. Results represent the mean ± SEM of at least three experiments. *p* values were calculated with Student's *t* test (* $p \leq 0.05$). Approximately 30 μg of protein lysate obtained from each tumor tissue and cell line was separated on 12% SDS-PAGE, and the equal protein loading was evaluated by GAPDH antibody probing in panels A and B.

overexpression of the NDUF8 was evident in HN8, HN12, and HN22 cells (Fig. 1B). Stimulation of complex I subunit expression could enhance OXPHOS, either to overcome a defect in another subunit or to support the high-energy demand in these HN cancer cell lines. On the other hand, the reduced expression of COII in HN8 cells could be due to defects in the expression of COII mRNA or mitochondrial translation machinery in this cell line. Another interesting observation is the reduced expression of this subunit in the HN8 but not the HN22 cell line, since these two cell lines were derived from the lymph node metastasis and the primary epiglottis squamous cell carcinoma of the same patient, respectively (Rajarajan et al., 2012). Therefore, we propose that the reduced COII expression could be adapted during the metastasis of squamous cell carcinoma in the lymph node of the same patient.

To further investigate the changes in COII mRNA expression, we performed semi-quantitative RT-PCR in HaCat and HN cell lines using the housekeeping gene GAPDH as a control (Fig. 1C). Clearly, the expression of COII mRNA was increased about 1.5–2 fold in HN cancer cell lines compared to the control HaCat cells, implying that the reduction in COII protein expression observed in HN8 cells was not due to decreased expression or stability of the COII mRNA. This observation also suggests that the reduced COII expression at the steady-state level (Fig. 1B) was not caused by a defect in the mitochondrial transcription machinery.

3.2. Mitochondrial translation is compromised in some of the head and neck cell lines

Next, we determined the de novo synthesis of 13 mitochondrial-encoded proteins in these cell lines using ^{35}S-Met pulse labeling in the presence of emetine (Fig. 2A). Emetine is an inhibitor of cytoplasmic protein synthesis and does not affect protein synthesis in mammalian mitochondria. In this analysis, the 13 essential OXPHOS subunits, de novo synthesized by mitochondrial ribosomes and translation machinery, were labeled by ^{35}S-Met (Fig. 2A). Clearly, there is an overall decrease in the incorporation of ^{35}S-Met into the 13 mitochondrial-encoded proteins in HN cancer cells, as the relative intensities of the labeled protein bands is much less in HN8 cell lines in comparison to the other cell lines (Fig. 2A and B). This observation is in agreement with the reduced expression of COII detected at the steady state level and also strongly suggests that mitochondrial translation or protein synthesis is impaired or defective in this cell line, which is derived from a lymph node metastasis of a stage IVA tumor of the oral pavement (Fig. 1B and Table 2) (Rajarajan et al., 2012).

3.3. Expression of MRPL11 is reduced in HNSCC tumors

The mitochondrial translation machinery, including translation factors and ribosomes, is essential for the synthesis of 13 mitochondrial-encoded components of the OXPHOS complexes (Christian and Spremulli, 2012; Koc et al., 2001b,c, 2010). The evidence we presented above also suggests that mitochondrial translation is impaired in HNSCC tumors and HN cancer cell lines (Fig. 1). In fact, transcripts of the two mitochondrial ribosomal proteins, MRPL11 and MRPL21, have been shown to be aberrantly expressed in microarray analyses of HNSCC tumors (Sugimoto et al., 2009). To determine the changes in the MRPL11 expression levels, we performed Western blot analysis of tumor samples. Not surprisingly, the expression of MRPL11 was clearly decreased in patient samples 3 and 4

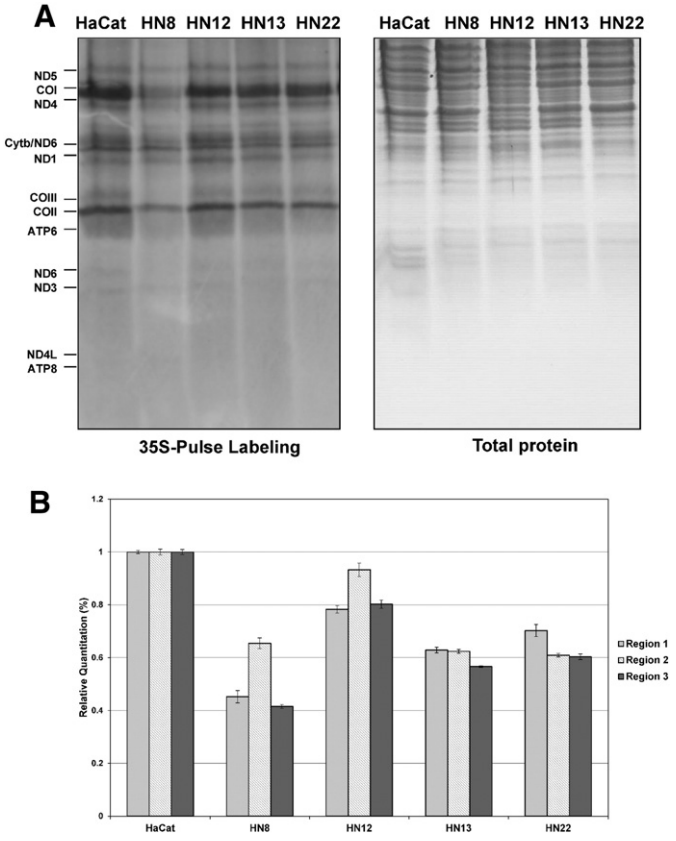

Fig. 2. A. Mitochondrial translation machinery is impaired in HN8 cells. A) De novo synthesis of 13 mitochondrial-encoded proteins was evaluated in control (HaCat) and HNSCC cells by pulse labeling of proteins in the presence of [^{35}S]-methionine and a cytosolic translation inhibitor, emetine. A representative electrophoretic pattern of the de novo synthesized translational products is presented. ND1, −2, −3, −4, −4 L, −5, and −6 are subunits of Complex I; Cyt *b* is a subunit of Complex III; COI, −II, and -III are subunits of Complex IV; ATP6 and ATP8 are subunits of Complex V. Coomassie blue staining of the same gel (total protein) was performed to ensure equal protein loading in the gel. B) The combined intensities of the 13 mitochondrial-encoded proteins shown in panel A were quantified as three different regions in each lane corresponding to the different cell lines. Regions 1–3 include ND5, COI, and ND4; Cytb, ND6, and ND1; and COIII, COII, and ATP6, respectively.

(Fig. 3A). This observation is in agreement with the decreased COII expression observed in patients 3 and 4 (Fig. 1A).

Changes in the expression of MRPL11 protein or mRNA through mutations or alternative splicing could result in the loss of mitochondrial translation activity and lead to reduction in the synthesis of mitochondrial-encoded proteins in HNSCC. To assess this possibility, we first quantitated the expression of the MRPL11 transcript in HN cell lines using qRT-PCR. In this analysis, MRPL11 mRNA levels in the HaCat cell line were used as a reference point, and its expression in HN cell lines was reported as the fold change of HaCat mRNA levels (Fig. 3B). Expression of the MRPL11 transcript in HN8 cells was reduced about two fold, which was less than that of the HaCat cell line (Fig. 3B). The increase in the MRPL11 transcript could potentially be a result of a defect in its function at the protein level. To compensate for defective MRPL11 protein activity, cells could stimulate its expression at its transcript. This hypothesis is consistent with the translation defect that we observed in the HN8 cell line, determined by ^{35}S-Met pulse labeling assay (Fig. 2A).

To correlate the changes observed in the MRPL11 transcript level to the protein expression level, Western blotting analyses were carried out in HaCat and HN cell lines. Remarkably, we detected a slight decrease in MRPL11 expression in the HN8 cell line compared to its expression in HaCat, HN13, HN12, and HN22 cell lines (Fig. 2B). In addition to the expression of MRPL11, we evaluated the expression of several other small and large subunit proteins in these cell lines. Although the translation defect we observed in the HN8 cell line (Figs. 1B and 2A) was more profound than the reduced expression of MRPs detected by Western blot analysis, it is still possible that another component of the mitochondrial translation machinery could be compromised in this cell line.

3.4. MRPL11 is essential for protein synthesis and OXPHOS in mammalian mitochondria

MRPL11 is one of the essential mitochondrial ribosomal proteins located in the L7/L12 stalk, as modeled in the crystal structure of the large subunit of the bacterial ribosome (Fig. 4A) (Koc et al., 2001c; Han et al., 2011; Greber et al., 2015). This region of the ribosome is involved in translation factor binding and/or recruitment during initiation, elongation, translocation, and termination to support the synthesis of 13 mitochondrial-encoded proteins in mammalian mitochondria (Christian and Spremulli, 2012; Amunts et al., 2015; Sharma et al., 2003). To demonstrate the essential role of MRPL11 in mitochondrial translation, we partially decreased MRPL11 expression in the HN12 cell line using siRNA directed against the MRPL11 transcript and performed ^{35}S-Met labeling of the de novo synthesized 13 mitochondrial proteins (Fig. 4B). The partial MRPL11 knockdown was determined by a Western blot analysis of the cell lysates, obtained from control and HN12 cells transfected with MRPL11 siRNA for only 24 h to prevent cell death (Fig. 4B). We observed about a 50% reduction in MRPL11 expression in cells transfected with MRPL11 siRNA, and this reduction coincided with the decreased expression of 13 mitochondrial proteins determined by ^{35}S-Met pulse labeling assay (Figs. 4B and 2). MRPL11 expression in the HN12 cell line was closer to its normal level in the HaCat cell line; however, its downregulation by siRNA created an effect on the expression of 13 mitochondrial proteins that was similar to their expression levels in HN8 cell lines, providing further evidence for mitochondrial translation defect(s) in the HN8 cell line. Again, we confirmed that MRPL11 is an essential protein and supports mitochondrial protein synthesis and regulates OXPHOS in mammalian mitochondria.

3.5. Cell growth and proliferation is possibly supported by aerobic glycolysis in HN8 cells

A switch in the energy metabolism from OXPHOS to aerobic glycolysis is one of the well-known hallmarks of cancer. At large, the initiation of this switch is attributed to mitochondrial dysfunction (Wallace, 2012; Sotgia et al., 2012; Chiavarina et al., 2012; Curry et al., 2013). In order to gain insights into the growth and proliferation of HN cells, we seeded an equal number of control HaCat and HN cancer cells and allowed them to grow for 72 h. The number of HN12 and HN22 cells was about 50% higher at the end of 72 h, whereas the number of cells or the cell growth rate was about the same for normal HaCat, HN8, and HN13 cells (Fig. 5A). These results were quite unexpected, since we observed about a 30–70% decrease in the synthesis of mitochondrial-encoded subunits of OXPHOS complexes in HN cells compared to the HaCat cell line (Figs. 1B and 2A). Surprisingly, the 70% decrease in the synthesis of these essential components in the HN8 cell line did not interfere with its growth rate. Therefore, we suggest that the HN8 cells were able to obtain the energy required for cell growth from aerobic glycolysis rather than OXPHOS due to a possible acquired defect in mitochondrial translation. The HN22 cell line, which is obtained from the primary squamous cell carcinoma of the same patient, could have partially used aerobic glycolysis, as its growth rate was higher than that of the control cells (Fig. 5A). However, mitochondrial translation and OXPHOS processes in these cells were fairly comparable to those of the control cells (Figs. 2A and 1B).

In addition to cell proliferation assays, we performed an in vitro wound-healing assay to evaluate the relative cell proliferation and migration of HN8, HN12, and HN22 cells. As seen in Fig. 5B, HN8 cells migrated approximately 70 μm from the edges and covered about 30% of the

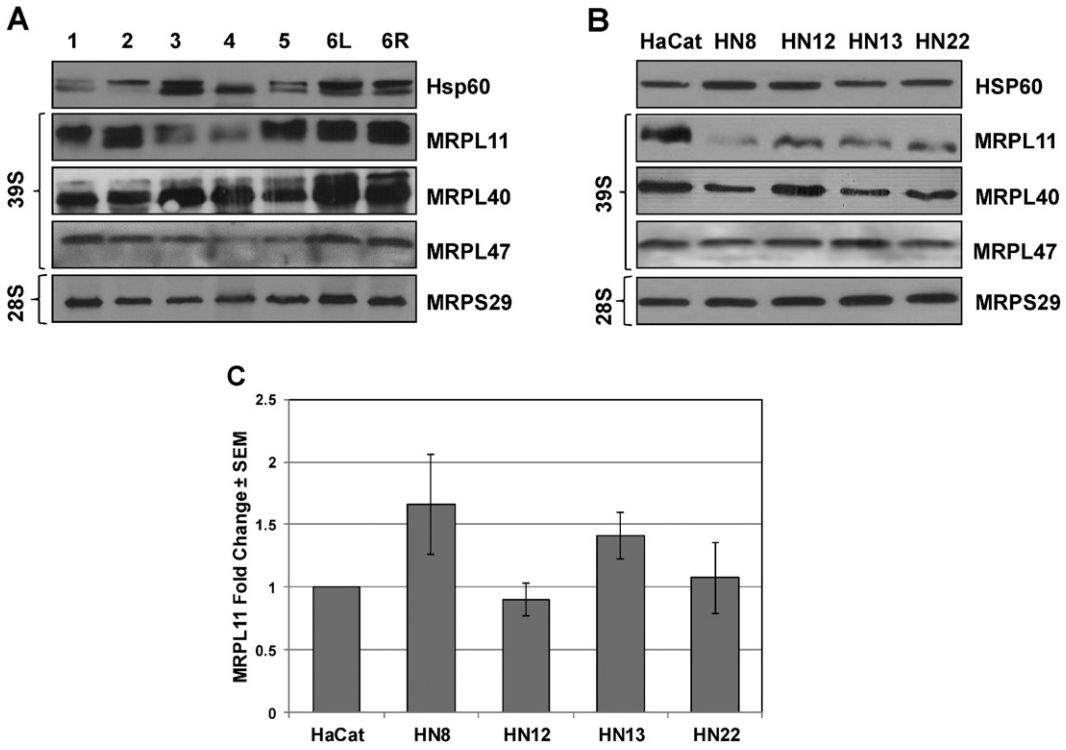

Fig. 3. MRPL11 expression is altered in human head and neck cancer tissues and HNSCC cell lines. A) MRPL11 protein expression was detected in total protein lysates obtained from seven human head and neck cancer biopsies by Western blot analysis. Samples, approximately 30 μg each, were separated on 12% SDS-PAGE, and membranes were probed with MRPL11 antibody. B) The expression of mitochondrial ribosomal protein MRPL11 and the other large subunit (39S) proteins (MRPL13, MRPL40, and MRPL47) and small subunit (28S) proteins (MRPS11 and MRPS29) in head and neck cancer and HaCat control cells was detected by Western blot analysis. Total cell lysates were separated on 12% SDS-PAGE and membranes were probed with specific MRP antibodies described in the Materials and Methods. Equal protein loading was ensured by HSP60 probing. C) Expression of the MRPL11 transcript was determined in HNSCC cell lines. Total RNA was extracted from HN8, HN12, HN13, and HN22 head and neck cancer cells and normal keratinocytes, HaCaT, as control. Real-Time RT-PCR was performed to study the relative changes in gene expression of MRPL11 relative to fold expression changes in β-Actin mRNA. Results represent the mean ± SEM of at least three experiments. *p* values were calculated with Student's *t* test on treated samples vs. CTRL VH (* $p \leq 0.05$).

scratch defect, while HN12 and HN22 cells almost completely covered the scratch defect. Again, this observation is in agreement with results obtained from the cell proliferation assay and points to dysfunctional mitochondrial translation and, therefore, OXPHOS in the HN8 cell line.

4. Discussion

The switch of energy metabolism from oxidative to aerobic glycolysis, possibly due to dysfunctional mitochondria, commonly known as the Warburg effect, was proposed to be one of the leading causes of tumor formation (Wallace, 2005, 2012). However, recent evidence suggests that tumor cells require a metabolically rich microenvironment to promote growth and metastasis (Wallace, 2012). To support this high metabolic demand and proliferation rate, these cells use oxidative metabolism for complete oxidation of glucose, which generates far more ATP than its oxidation to lactate in aerobic glycolysis (Sotgia et al., 2012; Chiavarina et al., 2012; Witkiewicz et al., 2012). In a recently proposed tumor metabolism model with at least two compartments, ROS generated by cancer cells with a high oxidative metabolism rate induce oxidative stress and aerobic glycolysis in tumor fibroblasts or stromal cells (Sotgia et al., 2012; Chiavarina et al., 2012; Witkiewicz et al., 2012). In fact, three metabolically different compartments have been reported in the mucosa of head and neck carcinoma, one of which contained mitochondria-rich proliferating tumor cells, while the other two were glycolytic non-proliferating tumor cells and stroma (Curry et al., 2013; Chatterjee et al., 2006; Carew and Huang, 2002). Because the complete oxidation of glucose and other metabolites, including lactate and ketone bodies, takes place in mitochondria via oxidative phosphorylation, having functional OXPHOS complexes is essential for this model of oxidative metabolism (Curry et al., 2013; Velez et al., 2013).

The mitochondrial genes encoding subunits of complex IV, COI, COII, and COIII, are found to be the most commonly mutated in HNSCCs (Challen et al., 2011; Zhou et al., 2007). In addition to these mtDNA mutations, the mitochondrial proteins encoded by nuclear genes responsible for mitochondrial biogenesis are also involved in HNSCC (Kim et al., 2006). Evidence also suggests that mutations and changes in expression and/or post-translational modifications of MRPs directly affect energy metabolism in mammalian mitochondria due to their roles in the synthesis of 13 mitochondrial-encoded proteins (Miller et al., 2004, 2008, 2009; Yang et al., 2010; Emdadul Haque et al., 2008; Smits et al., 2011; O'Brien et al., 2005; O'Brien, 2002). Interestingly, aberrant expression of the MRP genes, *MRPL11* and *MRPL21*, was detected among seven differentially expressed genes in 21 pairs of primary HNSCC tumors and 10 HNSCC cell lines using microarray analysis (Sugimoto et al., 2009). Changes in *MRPL11* expression was also correlated to metastatic uterine cervical cancer (Lyng et al., 2006).

In this study, we showed that the changes in expression of OXPHOS subunits, specifically, in one of the mitochondrial-encoded components of complex IV, COII, were associated with the changes in expression of MRPL11 at the protein level in tumor biopsies obtained from HNSCC and HNSCC cell lines (Figs. 1 and 2). MRPL11 is one of the mitochondrial ribosomal large subunit proteins that was more differentially expressed in the tumor tissues and cell lines tested. Its deletion resulted in the complete loss of the mitochondrial genome in *Saccharomyces Cerevisiae* (Zhang and Singh, 2014). This is not an unexpected observation, because

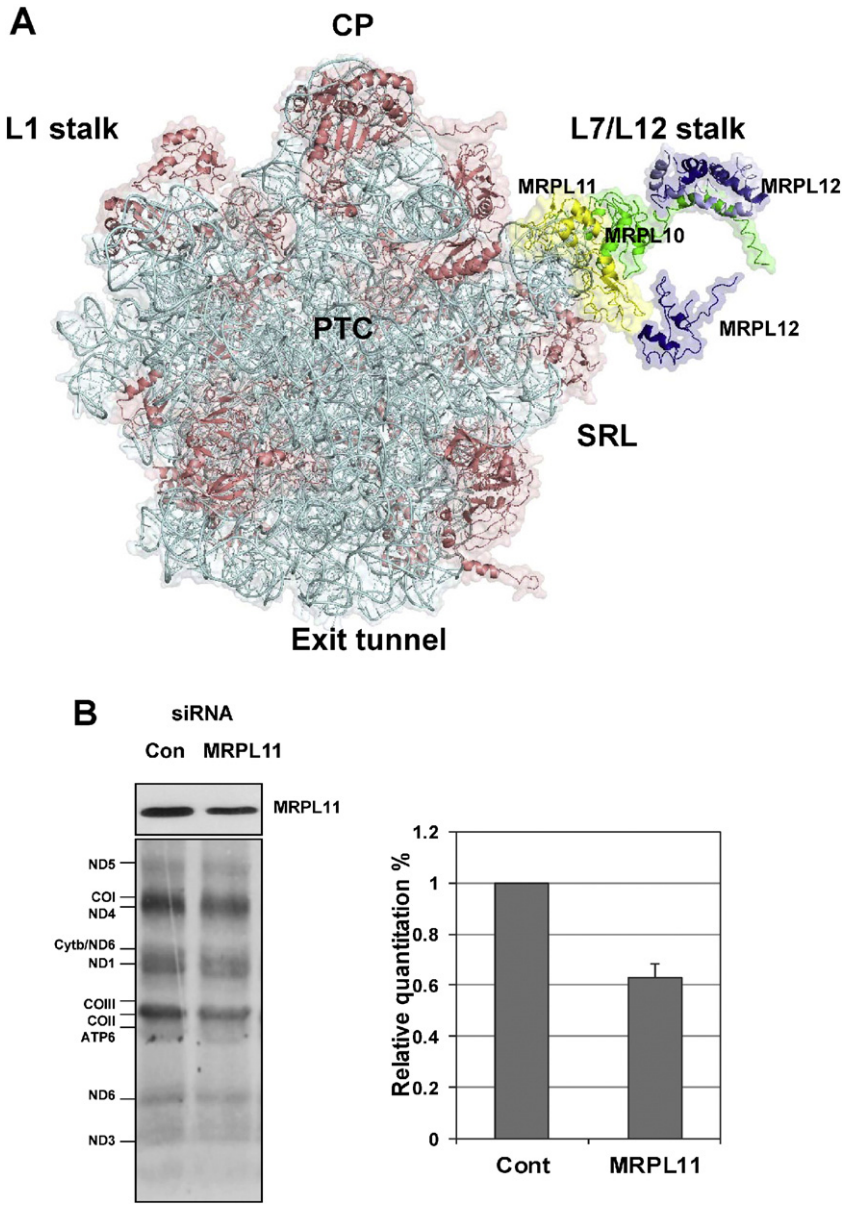

Fig. 4. MRPL11 is an essential mitochondrial ribosomal protein and regulates mitochondrial translation. A) MRPL11 is an essential mitochondrial ribosomal protein that forms the mitochondrial L7/L12 stalk along with MRPL10 and multiple copies of MRPL12. The mitochondrial L7/L12 stalk was modeled to indicate the locations of the mitochondrial L7/L12 stalk proteins MRPL10 (green), MRPL11 (yellow), and MRPL12 (blue) using the crystal structure, based on the bacterial large subunit (PDB# 2WRL). The large subunit rRNAs and proteins were colored in cyan and pink, respectively. Locations of functionally active sites of the large subunit, the peptidyl transferase center (PTC), sarcin–ricin loop (SRL), and L1 and L7/L12 stalks, are indicated in the structural model. The model was generated by PyMol software (DeLano Scientific LLC) (Brunger et al., 1998). B) Role of MRPL11 down regulation on mitochondrial protein synthesis. Expression of MRPL11 was determined in control and MRPL11 siRNA transfected HN12 cell lines by Western blotting (top panel). De novo synthesis of mitochondrial proteins was evaluated in control and MRPL11 knock-down cells by pulse labeling of proteins in the presence of [^{35}S]-methionine and a cytosolic translation inhibitor, emetine. A representative electrophoretic pattern of the de novo synthesized translational products is presented. ND1, −2, −3, −4, −4 L, −5, and −6 are subunits of Complex I; Cyt*b* is a subunit of Complex III; COI, -II, and -III are subunits of Complex IV; ATP6 and ATP8 are subunits of Complex V. The combined intensities of the 13 mitochondrial-encoded proteins from each lane were used as an overall quantitation of mitochondrial protein synthesis.

MRPL11 is located in an essential region of the ribosome that supports different stages of mitochondrial translation, including initiation, elongation, and termination. In fact, even a partial siRNA-dependent reduction in MRPL11 expression impaired mitochondrial translation in HN12 cell lines and influenced the expression of all the mitochondrial-encoded subunits of complex I, III, IV, and V (Fig. 4B). This is in agreement with the reduced expression of the 13 mitochondrial-encoded subunits in HN8 cell lines, determined by ^{35}S-Met pulse labeling assays (Fig. 2A). Similarly, a decrease in the steady-state expression of mitochondrial-encoded COII subunit and MRPL11 levels, as measured by Western blot, also supports a possible defect in mitochondrial translation in HN8 cells and tumor tissues obtained from patient 4 and to some extent in patient 3 (Fig. 1A and B). In addition to the decrease in the mitochondrial-encoded COII subunit in these patients, patient 1 has a significant decrease in one of the nuclear-encoded subunits of complex V (ATP5a) while patient 4 also has defects in the nuclear-encoded subunits of complex V, III, and I (Fig. 1A). Clearly, there is a strong correlation between the defects in expression of OXPHOS components and the advanced stage of HNSCC tumors, as all these patients had stage IVA tumors. In fact, patients 1, 3, and 4 were all affected by highly invasive oral cavity carcinomas, which were locally progressed and therefore involved adjacent tissues. In particular, complex V, III, IV, and I subunits were reduced significantly, in

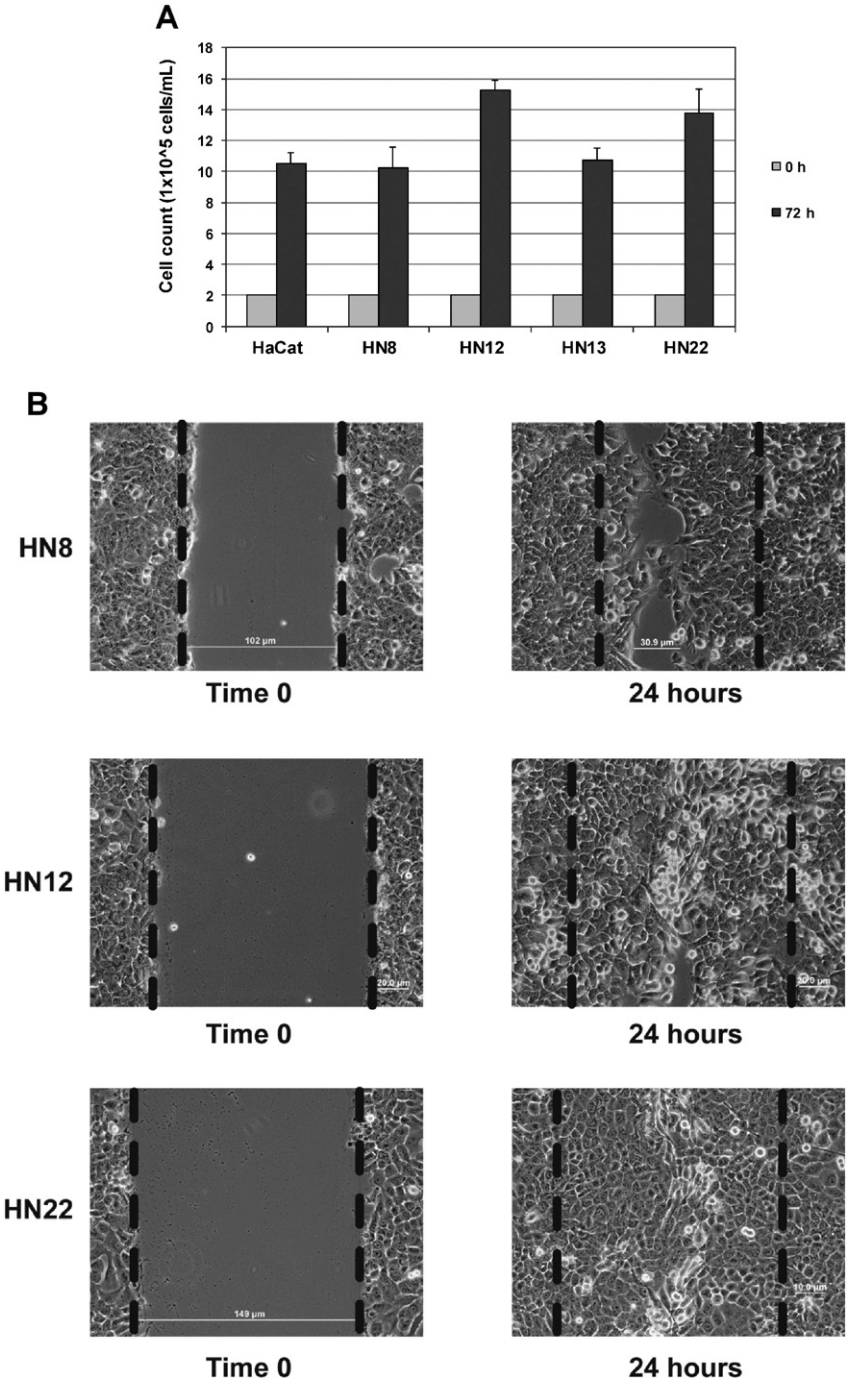

Fig. 5. Cell growth and proliferation is stimulated in head and neck cancer cells. A) Approximately 2×10^5 HaCat and head and neck cancer cells were seeded in triplicates of 6-well plates and incubated for 72 h. After this incubation period, cells were collected and counted. The results represent the mean ± SEM of at least three experiments. B) Wound-healing assays of HN8, HN12, and HN22 cells at 24 h. Inverted light microscope images of the HN cells at time 0 and 24 h are shown. Dashed lines represent scratch size at time 0 h. The magnification was set to 100×.

addition to the reduction of complex IV in the lysates from patient 4, who had several metastasis in multiple ipsilateral lymph nodes (pT4aN2bM0) (Table 1 and Fig. 1A). In patient 4, only the complex II subunits SDHB and SDHA were still expressed to partially support the mitochondrial activity (data not shown). This is possibly due to the composition of complex II, succinate dehydrogenase, which is formed by four nuclear-encoded subunits, SDHA, SDHB, SDHC, and SDHD. The presence of progressed disease, i.e., metastasis in multiple ipsilateral lymph nodes (patient 4), was correlated with the reduced expression of MRPL11 and the mitochondrial subunit COII. Inhibition of mitochondrial translation by reduced expression of MRPL11 not only reduced the 13 mitochondrial proteins but also decreased the expression of nuclear-encoded subunits of OXPHOS complexes I, III, IV, and V in the same patient (patient 4, Figs. 1A and 3A). As described above, the HN8 cell line, which was obtained from a stage IVA patient with multiple metastatic lymph nodes (Table 2), also showed reduced expression of MRPL11 and mitochondrial-encoded subunit COII (Fig. 1B and C). However, the paired HN22 cell line derived from the primary tumor of the same patient expressed a comparable level of MRPL11 and of the 13 mitochondrial translation products with the other cell lines tested (Figs. 1B and 3B).

Altogether, we can infer from these observations that the defects in mitochondrial translation and energy metabolism could be responsible for stimulation of cell proliferation rates in HNSCC and HN cell lines. Future research is expected to demonstrate that the

detection of changes in the expression of OXPHOS components, and MRPL11 levels, and components of mitochondrial translation machinery may be used as markers for HNSCC tumor staging and indicators of cancer progression.

Acknowledgments

The authors would like to thank Ms. Tamara Murphy and Dr. Candace M. Howard for their valuable contributions in the preparation of this manuscript. We also gratefully acknowledge the Marshall University School of Medicine Biochemistry and Microbiology Department for its support.

References

Amunts, A., Brown, A., Toots, J., Scheres, S.H., Ramakrishnan, V., 2015. Ribosome. The structure of the human mitochondrial ribosome. Science 348, 95–98.
Brandon, M., Baldi, P., Wallace, D.C., 2006. Mitochondrial mutations in cancer. Oncogene 25, 4647–4662.
Brunger, A.T., Adams, P.D., Clore, G.M., DeLano, W.L., Gros, P., Grosse-Kunstleve, R.W., Jiang, J.S., Kuszewski, J., Nilges, M., Pannu, N.S., et al., 1998. Crystallography & NMR system: a new software suite for macromolecular structure determination. Acta Crystallogr. D Biol. Crystallogr. 54, 905–921.
Carew, J.S., Huang, P., 2002. Mitochondrial defects in cancer. Mol. Cancer 1, 9.
Carim, L., Sumoy, L., Nadal, M., Estivill, X., Escarceller, M., 1999. Cloning, expression, and mapping of PDCD9, the human homolog of *Gallus gallus* pro-apoptotic protein p52. Cytogenet. Cell Genet. 87, 85–88.
Cavalieri, D., Dolara, P., Mini, E., Luceri, C., Castagnini, C., Toti, S., Maciag, K., De Filippo, C., Nobili, S., Morganti, M., et al., 2007. Analysis of gene expression profiles reveals novel correlations with the clinical course of colorectal cancer. Oncol. Res. 16, 535–548.
Challen, C., Brown, H., Cai, C., Betts, G., Paterson, I., Sloan, P., West, C., Birch-Machin, M., Robinson, M., 2011. Mitochondrial DNA mutations in head and neck cancer are infrequent and lack prognostic utility. Br. J. Cancer 104, 1319–1324.
Chandra, D., Singh, K.K., 2011. Genetic insights into OXPHOS defect and its role in cancer. Biochim. Biophys. Acta 1807, 620–625.
Chatterjee, A., Mambo, E., Sidransky, D., 2006. Mitochondrial DNA mutations in human cancer. Oncogene 25, 4663–4674.
Chiavarina, B., Martinez-Outschoorn, U.E., Whitaker-Menezes, D., Howell, A., Tanowitz, H.B., Pestell, R.G., Sotgia, F., Lisanti, M.P., 2012. Metabolic reprogramming and two-compartment tumor metabolism: opposing role(s) of HIF1alpha and HIF2alpha in tumor-associated fibroblasts and human breast cancer cells. Cell Cycle 11, 3280–3289.
Christian, B.E., Spremulli, L.L., 2012. Mechanism of protein biosynthesis in mammalian mitochondria. Biochim. Biophys. Acta 1819, 1035–1054.
Curry, J.M., Tuluc, M., Whitaker-Menezes, D., Ames, J.A., Anantharaman, A., Butera, A., Leiby, B., Cognetti, D.M., Sotgia, F., Lisanti, M.P., et al., 2013. Cancer metabolism, stemness and tumor recurrence: MCT1 and MCT4 are functional biomarkers of metabolic symbiosis in head and neck cancer. Cell Cycle 12, 1371–1384.
Dasgupta, S., Koch, R., Westra, W.H., Califano, J.A., Ha, P.K., Sidransky, D., Koch, W.M., 2010. Mitochondrial DNA mutation in normal margins and tumors of recurrent head and neck squamous cell carcinoma patients. Cancer Prev. Res. (Phila.) 3, 1205–1211.
Emdadul Haque, M., Grasso, D., Miller, C., Spremulli, L.L., Saada, A., 2008. The effect of mutated mitochondrial ribosomal proteins S16 and S22 on the assembly of the small and large ribosomal subunits in human mitochondria. Mitochondrion 8, 254–261.
Greber, B.J., Bieri, P., Leibundgut, M., Leitner, A., Aebersold, R., Boehringer, D., Ban, N., 2015. The complete structure of the 55S mammalian mitochondrial ribosome. Science 348, 303–308.
Han, M.J., Chiu, D.T., Koc, E.C., 2010. Regulation of mitochondrial ribosomal protein S29 (MRPS29) expression by a 5′-upstream open reading frame. Mitochondrion 10, 274–283.
Han, M.J., Cimen, H., Miller-Lee, J.L., Koc, H., Koc, E.C., 2011. Purification of human mitochondrial ribosomal L7/L12 stalk proteins and reconstitution of functional hybrid ribosomes in *Escherichia coli*. Protein Expr. Purif. 78, 48–54.
Hanahan, D., Weinberg, R.A., 2011. Hallmarks of cancer: the next generation. Cell 144, 646–674.
Huang, Y., Ballinger, D.G., Dai, J.Y., Peters, U., Hinds, D.A., Cox, D.R., Beilharz, E., Chlebowski, R.T., Rossouw, J.E., McTiernan, A., et al., 2011. Genetic variants in the MRPS30 region and postmenopausal breast cancer risk. Genome Med. 3, 42.
Jeon, G.A., Lee, J.S., Patel, V., Gutkind, J.S., Thorgeirsson, S.S., Kim, E.C., Chu, I.S., Amornphimoltham, P., Park, M.H., 2004. Global gene expression profiles of human head and neck squamous carcinoma cell lines. Int. J. Cancer 112, 249–258.
Kim, M.M., Glazer, C.A., Mambo, E., Chatterjee, A., Zhao, M., Sidransky, D., Califano, J.A., 2006. Head and neck cancer cell lines exhibit differential mitochondrial repair deficiency in response to 4NQO. Oral Oncol. 42, 201–207.
Kissil, J.L., Deiss, L.P., Bayewitch, M., Raveh, T., Khaspekov, G., Kimchi, A., 1995. Isolation of DAP3, a novel mediator of interferon-gamma-induced cell death. J. Biol. Chem. 270, 27932–27936.
Koc, E.C., Ranasinghe, A., Burkhart, W., Blackburn, K., Koc, H., Moseley, A., Spremulli, L.L., 2001a. A new face on apoptosis: death-associated protein 3 and PDCD9 are mitochondrial ribosomal proteins. FEBS Lett. 492, 166–170.
Koc, E.C., Burkhart, W., Blackburn, K., Moseley, A., Spremulli, L.L., 2001b. The small subunit of the mammalian mitochondrial ribosome: identification of the full complement of ribosomal proteins present. J. Biol. Chem. 276, 19363–19374.
Koc, E.C., Burkhart, W., Blackburn, K., Moyer, M.B., Schlatzer, D.M., Moseley, A., Spremulli, L.L., 2001c. The large subunit of the mammalian mitochondrial ribosome. Analysis of the complement of ribosomal proteins present. J. Biol. Chem. 276, 43958–43969.
Koc, E.C., Cimen, H., Kumcuoglu, B., Abu, N., Akpinar, G., Haque, M.E., Spremulli, L.L., Koc, H., 2013. Identification and characterization of CHCHD1, AURKAIP1, and CRIF1 as new members of the mammalian mitochondrial ribosome. Front. Physiol. 4, 183.
Koc, E.C., Haque, M.E., Spremulli, L.L., 2010. Current views of the structure of the mammalian mitochondrial ribosome. Isr. J. Chem. 50, 45–59.
Levshenkova, E.V., Ukraintsev, K.E., Orlova, V.V., Alibaeva, R.A., Kovriga, I.E., Zhugdernamzhilyn, O., Frolova, E.I., 2004. The structure and specific features of the cDNA expression of the human gene MRPL37. Bioorg. Khim. 30, 499–506.
Lyng, H., Brovig, R.S., Svendsrud, D.H., Holm, R., Kaalhus, O., Knutstad, K., Oksefjell, H., Sundfor, K., Kristensen, G.B., Stokke, T., 2006. Gene expressions and copy numbers associated with metastatic phenotypes of uterine cervical cancer. BMC Genomics 7, 268.
Miller, C., Saada, A., Shaul, N., Shabtai, N., Ben-Shalom, E., Shaag, A., Hershkovitz, E., Elpeleg, O., 2004. Defective mitochondrial translation caused by a ribosomal protein (MRPS16) mutation. Ann. Neurol. 56, 734–738.
Miller, J.L., Koc, H., Koc, E.C., 2008. Identification of phosphorylation sites in mammalian mitochondrial ribosomal protein DAP3. Protein Sci. 17, 251–260.
Miller, J.L., Cimen, H., Koc, H., Koc, E.C., 2009. Phosphorylated proteins of the mammalian mitochondrial ribosome: implications in protein synthesis. J. Proteome Res. 8, 4789–4798.
Milne, R.L., Gaudet, M.M., Spurdle, A.B., Fasching, P.A., Couch, F.J., Benitez, J., Arias Perez, J.I., Zamora, M.P., Malats, N., Dos Santos Silva, I., et al., 2010. Assessing interactions between the associations of common genetic susceptibility variants, reproductive history and body mass index with breast cancer risk in the breast cancer association consortium: a combined case–control study. Breast Cancer Res. 12, R110.
Mukamel, Z., Kimchi, A., 2004. Death-associated protein 3 localizes to the mitochondria and is involved in the process of mitochondrial fragmentation during cell death. J. Biol. Chem. 279, 36732–36738.
O'Brien, T.W., 2002. Evolution of a protein-rich mitochondrial ribosome: implications for human genetic disease. Gene 286, 73–79.
O'Brien, T.W., O'Brien, B.J., Norman, R.A., 2005. Nuclear MRP genes and mitochondrial disease. Gene 354, 147–151.
Rajarajan, A., Stokes, A., Bloor, B.K., Ceder, R., Desai, H., Grafstrom, R.C., Odell, E.W., 2012. CD44 expression in oro-pharyngeal carcinoma tissues and cell lines. PLoS One 7, e28776.
Sharma, M.R., Koc, E.C., Datta, P.P., Booth, T.M., Spremulli, L.L., Agrawal, R.K., 2003. Structure of the mammalian mitochondrial ribosome reveals an expanded functional role for its component proteins. Cell 115, 97–108.
Smits, P., Saada, A., Wortmann, S.B., Heister, A.J., Brink, M., Pfundt, R., Miller, C., Haas, D., Hantschmann, R., Rodenburg, R.J., et al., 2011. Mutation in mitochondrial ribosomal protein MRPS22 leads to Cornelia de Lange-like phenotype, brain abnormalities and hypertrophic cardiomyopathy. Eur. J. Hum. Genet. 19, 394–399.
Sotgia, F., Whitaker-Menezes, D., Martinez-Outschoorn, U.E., Salem, A.F., Tsirigos, A., Lamb, R., Sneddon, S., Hulit, J., Howell, A., Lisanti, M.P., 2012. Mitochondria "fuel" breast cancer metabolism: fifteen markers of mitochondrial biogenesis label epithelial cancer cells, but are excluded from adjacent stromal cells. Cell Cycle 11, 4390–4401.
Stacey, S.N., Manolescu, A., Sulem, P., Thorlacius, S., Gudjonsson, S.A., Jonsson, G.F., Jakobsdottir, M., Bergthorsson, J.T., Gudmundsson, J., Aben, K.K., et al., 2008. Common variants on chromosome 5p12 confer susceptibility to estrogen receptor–positive breast cancer. Nat. Genet. 40, 703–706.
Sugimoto, T., Seki, N., Shimizu, S., Kikkawa, N., Tsukada, J., Shimada, H., Sasaki, K., Hanazawa, T., Okamoto, Y., Hata, A., 2009. The galanin signaling cascade is a candidate pathway regulating oncogenesis in human squamous cell carcinoma. Genes Chromosom. Cancer 48, 132–142.
Velez, J., Hail Jr., N., Konopleva, M., Zeng, Z., Kojima, K., Samudio, I., Andreeff, M., 2013. Mitochondrial uncoupling and the reprograming of intermediary metabolism in leukemia cells. Front. Oncol. 3, 67.
Wallace, D.C., 2005. Mitochondria and cancer: Warburg addressed. Cold Spring Harb. Symp. Quant. Biol. 70, 363–374.
Wallace, D.C., 2012. Mitochondria and cancer. Nat. Rev. Cancer 12, 685–698.
Witkiewicz, A.K., Whitaker-Menezes, D., Dasgupta, A., Philp, N.J., Lin, Z., Gandara, R., Sneddon, S., Martinez-Outschoorn, U.E., Sotgia, F., Lisanti, M.P., 2012. Using the "reverse Warburg effect" to identify high-risk breast cancer patients: stromal MCT4 predicts poor clinical outcome in triple-negative breast cancers. Cell Cycle 11, 1108–1117.
Yang, Y., Cimen, H., Han, M.J., Shi, T., Deng, J.H., Koc, H., Palacios, O.M., Montier, L., Bai, Y., Tong, Q., et al., 2010. NAD+-dependent deacetylase SIRT3 regulates mitochondrial protein synthesis by deacetylation of the ribosomal protein MRPL10. J. Biol. Chem. 285, 7417–7429.
Yoo, Y.A., Kim, M.J., Park, J.K., Chung, Y.M., Lee, J.H., Chi, S.G., Kim, J.S., Yoo, Y.D., 2005. Mitochondrial ribosomal protein L41 suppresses cell growth in association with p53 and p27Kip1. Mol. Cell. Biol. 25, 6603–6616.
Zhang, H., Singh, K.K., 2014. Global genetic determinants of mitochondrial DNA copy number. PLoS One 9, e105242.
Zhou, S., Kachhap, S., Sun, W., Wu, G., Chuang, A., Poeta, L., Grumbine, L., Mithani, S.K., Chatterjee, A., Koch, W., et al., 2007. Frequency and phenotypic implications of mitochondrial DNA mutations in human squamous cell cancers of the head and neck. Proc. Natl. Acad. Sci. U. S. A. 104, 7540–7545.